Layering of surface snow and firn at Kohnen Station, Antarctica – noise or seasonal signal?

Thomas Laepple[1], Maria Hörhold[2,3], Thomas Münch[1,5], Johannes Freitag[4], Anna Wegner[4], Sepp Kipfstuhl[4]

[1]Alfred Wegener Institute Helmholtz Centre for Polar and Marine Research, Telegrafenberg A43, 14473 Potsdam, Germany

[2]Institute of Environmental Physics, University of Bremen, Otto-Hahn-Allee 1, D-28359 Bremen

[3]now at Alfred Wegener Institute Helmholtz Centre for Polar and Marine Research, Am Alten Hafen 26, 27568 Bremerhaven, Germany

[4]Alfred Wegener Institute Helmholtz Centre for Polar and Marine Research, Am Alten Hafen 26, 27568 Bremerhaven, Germany

[5]Institute of Physics and Astronomy, University of Potsdam, Karl-Liebknecht-Str. 24/25, 14476 Potsdam, Germany

Corresponding author: Thomas Laepple (tlaepple@awi.de)

- Extensive dataset of vertical and horizontal firn density variations at EDML, Antarctica
- Even in low accumulation regions, the density in the upper firn exhibits a seasonal cycle
- Strong stratigraphic noise masks the seasonal cycle when analyzing single firn cores

Abstract

The density of firn is an important property for monitoring and modeling the ice sheet as well as to model the pore close-off and thus to interpret ice core-based greenhouse gas records. One feature, which is still in debate, is the potential existence of an annual cycle of firn density in low-accumulation regions. Several studies describe or assume seasonally successive density layers, horizontally evenly distributed, as seen in radar data. On the other hand, high-resolution density measurements on firn cores in Antarctica and Greenland showed no clear seasonal cycle in the top few meters. A major caveat of most existing snow-pit and firn-core based studies is that they represent one vertical profile from a laterally heterogeneous density field. To overcome this, we created an extensive dataset of horizontal and vertical density data at Kohnen Station, Dronning Maud Land on the East Antarctic Plateau. We drilled and analyzed three 90 m long firn cores as well as 160 one meter long vertical profiles from two elongated snow trenches to obtain a two dimensional view of the density variations. The analysis of the 45 m wide and 1m deep density fields reveals a seasonal cycle in density. However, the seasonality is overprinted by strong stratigraphic noise, making it invisible when analyzing single firn cores. Our density dataset extends the

This article has been accepted for publication and undergone full peer review but has not been through the copyediting, typesetting, pagination and proofreading process which may lead to differences between this version and the Version of Record. Please cite this article as doi: 10.1002/2016JF003919

view from the local ice-core perspective to a hundred meter scale and thus supports linking spatially integrating methods such as radar and seismic studies to ice and firn cores.

1 Introduction

Density, as a physical property of polar firn, is important for many topics of polar research. The determination of the ice sheets mass balance by either modelling or monitoring of the ice sheets with ground-penetrating radar or with satellite laser altimetry is strongly related to firn density [*Rott et al.*, 1993; *Li and Zwally*, 2002; *Rotschky et al.*, 2006]. The evolution of the firn density further determines the air enclosure in ice at the firn-ice transition [*Martinerie et al.*, 1992; *Schwander et al.*, 1997].

Polar firn is characterized by layering, each layer generated by a single deposition event and associated with different physical properties. The resulting vertical density variability caused by this layering is responsible for the depth and time when air trapped in the firn and ice is sealed off from the exchange with the atmosphere, thereby determining the age difference between air bubbles in ice cores and their surrounding ice [*Landais et al.*, 2006; *Mitchell et al.*, 2015]. It was previously demonstrated that the layering changes with depth, showing a seasonal cyclicity in depths below 20-30 m that is highly correlated with seasonally varying impurity concentration [*Hörhold et al.*, 2012; *Freitag et al.*, 2013a]. It is speculated since then that impurities, featuring a seasonal cycle in their concentration, reshape the layering by changing the mechanical properties of the snow and the firn and thus influence the densification of single layers [*Hörhold et al.*, 2012; *Freitag et al.*, 2013a; *Fujita et al.*, 2014; *Gregory et al.*, 2014].

The horizontal and vertical density variability at the surface of ice-sheets is unclear. On one hand, radar images suggest an image of layers that undulate at a kilometer-scale but are nevertheless continuous [*Arcone et al.*, 2005; *Anschütz et al.*, 2007; *Arthern et al.*, 2013]. Thus, the firn column on top of the ice sheets is often understood as a sequence of successive layers [*Gow*, 1965; *Palais*, 1984; *Kreutz et al.*, 1999]. Accumulation rates extracted from ground-penetrating radar or satellite images are one example for this concept of successive horizontally distributed annual layers [*Winebrenner et al.*, 2001; *Anschütz et al.*, 2007; *Eisen et al.*, 2008; *Arthern et al.*, 2013]. The concept of annual layer deposition is further more supported by measurements of impurity concentrations or stable water isotopes, which exhibit a seasonal cycle in the atmosphere prior to deposition. These properties show a seasonal cycle within the snow and firn at many polar sites [*Gow*, 1965; *Benson*, 1971; *Palais*, 1984; *Alley*, 1988; *Goektas et al.*, 2002; *Svensson et al.*, 2015], suggesting homogenous formation of successive layers throughout each year. On the other hand, especially in low-accumulation regions, considerable horizontal variability is observed [*Libois et al.*, 2015]. This is reflected by the different stratification found in nearby snow pits [*Fisher et al.*, 1985; *Karlöf et al.*, 2006]. Further, high resolution density analysis of firn-core material [*Hörhold et al.*, 2012; *Freitag et al.*, 2013a] did not reveal a seasonal cycle in the surface firn density suggesting that re-deposition and wind-scouring dominate over the successive deposition of seasonal layers.

In this manuscript, we reconcile the previous findings of a lack in seasonality in the top meters of firn cores with the observed large-scale seasonal layering of the firn. Analyzing density on vertical and horizontal scales from the cm to the 100 m scale, we demonstrate that the question of layering and seasonality depends on the analyzed spatial scale.

2 Materials and Methods

In austral summer 2012/2013, close to the EPICA Dronning Maud Land drill site (EDML), firn cores and trenches were sampled and analyzed for density (Fig. 1). The site is characterized by a mean temperature of -44.5 °C and a mean accumulation rate of 62-73 kg/m^2/year depending on the age-interval used in the accumulation estimate [*Oerter et al.*, 2004; *Klein*, 2014]. The isotope data of the trenches are described in Muench et al., [2016].

2.1 Density profiles from firn cores

Four firn cores of at least 90 m length were drilled in the close vicinity of the EDML deep-drilling site and analyzed for density variations. We include three of the cores in this study (Fig. 1) as the core quality of the first core of the season (B40) was considerably lower than for the remaining cores. The firn cores were transported in 1 m pieces to the cold laboratory at the Alfred-Wegener-Institute (AWI) in Bremerhaven, Germany. Density of the firn cores was measured at a 0.5 mm resolution using high-resolution X-ray Computer Tomography (CT) [*Freitag et al.*, 2013a].

2.2 2D density profiles from shallow firn trenches

To study the horizontal density structure, close to the firn core positions, two 1.2 m deep, 1.2 m wide and around 45 m long trenches named T1 and T2 were excavated using a snow blower (Table 1). Each trench was directed perpendicularly to the local snow-dune direction. In contrast to other studies, the vertical zero position for each trench was not set to the snow-surface, but an absolute height reference was defined as a horizontal line between the highest points of the surface level of each trench. This was established using short bamboo poles every 60 cm, aligned by a spirit level and a laser device. Unfortunately, due to technical problems, no absolute height reference between the two trenches could be established. A coarse measurement based on stacked laser level measurements showed that the vertical difference between the trenches is less than 20 cm.

Every 60 cm, 1 m long firn cores were taken by carefully pushing a glass fiber liner with 98mm diameter vertically into the firn at ~5-10 cm distance to the trench wall. The full liners were carefully recovered by digging them out. During the process of pushing the liners into the snow, care was taken that the snow inside the liner did not get compressed. Liners with more than 1cm compression, visible as a reduction of the snow level at the top relative to its surroundings, were remeasured by moving the position 15 cm perpendicularly to the trench wall. In some cases, the replicate measurements again showed compression and thus no data could be obtained for this position. The vertical distance from the top of the liner to the absolute reference was recorded with an accuracy of 1 cm. The snow-filled liners were carefully transported to the EDML processing trench.

2.3 Dielectric profiling and density estimates.

The dielectric stratigraphy was measured in the processing trench applying the dielectric profiling (DEP) technique using the device described in Wilhelms et al. [1998]. Measurements were performed at 250 kHz frequency in 5 mm increments. The effective resolution is limited by the finite width of the one-cm wide electrode and was found to be around 2 cm based on analyzing the air to ice transition at the top of the core.

The top and bottom 4 cm of the DEP measurements are affected by edge-effects due to the air to ice transition. Sometimes, a loss of snow at the top or bottom of the liner in the packing or transporting phase could not be completely avoided. The maximum-recorded loss was 4 cm at the top and 1cm at the bottom. We therefore only analyze the part from 8-95 cm depth. For

each measurement, the cable stray capacitance was subtracted and the capacitance record was divided by the free air capacitance, to derive the relative permittivity. To convert the DEP measurements into density, we use the real valued Looyenga mixing model [Looyenga, 1965].

$$\varrho = \varrho_{ice} \frac{\varepsilon^{1/3} - 1}{{\varepsilon_{ice}}^{1/3} - 1}$$

where $\varrho_{ice} = 920 \frac{kg}{m^3}$ is the density of pure ice and $\varepsilon_{ice} = 3.17$ is the relative permittivity of ice at frequencies above 100 kHz [Glen and Paren, 1975]. This mixing model is a good approximation in the top meters of the firn and a comparison to gamma-ray based density measurements showed deviations of less than 5% in the top 40 m of a firn core [*Wilhelms*, 1996].

2.4 Comparison of DEP-derived density and CT density

It is known that effects other than density also influence the dielectric stratigraphy including strong impurity changes or changes in the snow structure [*Denoth*, 1989]. Further, CT-derived densities have a true resolution of 0.5 mm, whereas DEP-derived densities are always integrated over a width of several millimeters and are more sensitive to core breaks.

As we use both density measurement techniques in our study, we tested comparability of the methods by comparing the CT- and DEP-derived density for the firn core B41 (Fig. 2). We analyzed the top 10 m for they cover a similar density range (250-550 kg/m^3) as found in the trench. CT-derived densities were smoothed over 25 mm using a 50-point running mean filter to result in a comparable resolution. In the remaining manuscript, we will always use the 25 mm running mean smoothed CT data except for the spectral analysis, which is performed on the raw data.

Both methods show a strong agreement in variations on the cm to meter scale (R^2=0.91). A small offset (12 kg/m^3 difference in the 0-10 m mean density) between the CT and DEP density is observed, with the DEP showing a smaller density than the CT but this does not affect our results as we only rely on relative density variations in this study

The main deviations occur at core breaks and at the boundary of the 1m pieces. By integrating over several cm, the DEP device is more sensitive to small geometrical deviations from core-catchers and breaks than the CT measurements. As the trench DEP measurements were performed using firn inside liners, the firn/snow is better preserved and we expect a higher quality of the DEP-derived density of the trenches compared to the firn core results shown here.

2.5. Ion Measurements

Within trench T2, discrete sampling at core positions 0.3, 10, 29.80 and 40 m (distance along the trench) was conducted. The snow surface was cleaned by removing the outer most layers. The snow was sampled in 3 cm increments and collected in Whirlpak plastic bags using a pre-cleaned Teflon spatula. The samples were closed carefully and sealed again for transportation back to Germany. During sampling protective Tyvek cloths were worn to avoid contamination. Samples were shipped in cool containers to Bremerhaven, Germany, and kept frozen until analysis.

The analyses of the samples were carried out in the Ion Chromatography laboratory facilities at AWI using DIONEX IC-S 2100. Blanks were checked regularly and typically showed below 0.6 ppb for Na^+ and below the detection limit for methyl sulphonate (MSA). The ions of Na^+ and MSA are presented here. Ca^{2+} measurements suffer from contamination and are thus not included in the analysis. Because impurity concentrations are always positive but show an asymmetry towards large values [e.g. *Bigler et al.*, 2011], we use the logarithm of the ion concentration in all cases.

3 Results

3.1 2D density data from the trenches

The large number (160) of density profiles analyzed from the two trenches allows creating a two-dimensional image of the horizontal and vertical density variations (Fig. 3). The density distribution in both trenches shows a high vertical and horizontal variability with very similar magnitudes in both dimensions ($sd_{vertical}$ = 20.7 kg/m^3, $sd_{horizontal}$=19.7 kg/m^3).

Roughly four layers can be identified as alternations of high and low-density regions. Interestingly, as previously found while analyzing the isotope data from trench T1 [*Muench et al.*, 2016], the density layers below 30 cm seem to be on average horizontal and do not follow the actual snow surface. Indicative for this behavior is the smaller horizontal variability below 30 cm when all profiles are aligned to an absolute height (sd=17.8 kg/m^3) compared to the horizontal variability relative to the snow surface (sd=20.1 kg/m^3). Therefore, in the remainder of this study, we use and display the profiles relative to an absolute height reference and not to the snow surface.

The layers show undulations of several centimeters, similar in magnitude to the surface undulations that were present during the time of the sampling. Some density variations could be explained by vertically compressing or stretching the same density profile. However, in addition other features are visible. Prominent are high-density anomalies (400-420 kg/m^3) with a horizontal extension of 2-5 m, which are especially frequent in the 20-70 cm firn depth range.

3.2 Correlation structure of trench and firn core data

To visualize the density variability and representativity of single profiles, we show four arbitrarily picked density profiles from the trenches T1 and T2 together with the density profiles of the top 5 m from the firn cores (Fig. 4). This mimics the results we would have obtained in a classical study analyzing single snow-pits or firn cores. The first meter does not show an increase in density. Furthermore, no clear seasonal cycle is visible in the uppermost meter. Interestingly, all shown density profiles are uncorrelated to each other ($R<0.2$ for all possible correlation pairs) demonstrating that the density profile of a single core is not representative for a larger region, at least on the vertical cm to meter scale shown here.

Similar results are obtained from analyzing all profiles by correlating all the possible pairs of individual profiles from trench T1 with individual profiles from T2. This results in a mean correlation of 0.0. Allowing for a shift in the depth of +-12 cm for every single profile, and thus for potential undulations of the present snow surface, increases the mean correlation to 0.31. However, this is roughly what is expected by chance ($R=0.28$ using surrogate data with the same autocorrelation structure as the sample autocorrelation of the real data) since allowing for shifts always leads to spurious positive correlations.

While these horizontally separated profiles are uncorrelated, a different picture is obtained for nearby profiles. Estimating the correlation for different separation distances (Fig. 5) shows that nearby (<1 m distance) firn profiles are highly correlated (R=0.65) but this correlation drops to ~0.13 for separation distances larger than 10 m.

3.3 Mean profiles and comparison to water isotopes and ion concentrations

To reduce the local variability, we average all profiles inside each trench to obtain a mean density profile for each of the two trenches (Fig 6a). Interestingly, whereas single profiles between both trenches are uncorrelated, the mean profiles are highly reproducible (R=0.83) when allowing for a 6 cm depth shift, which is well inside the relative vertical alignment uncertainty of both trenches. This demonstrates that the profiles contain a signal representative at least over a 500 m scale.

To learn about the timing of the density variations, we additionally show the mean $\delta^{18}O$ profiles based on 38 profiles in trench T1 and 4 profiles in trench T2 (Fig. 6b and c) [*Muench et al.*, 2016]. In both trenches, $\delta^{18}O$ and density variations show a weak but significant positive correlation (R=0.34 and 0.31). High $\delta^{18}O$ values correspond to higher densities and vice versa. However, there are also considerable differences between both parameters, especially below 60cm where the density shows a minimum not represented in $\delta^{18}O$. Both trenches suggest a slight (depth) lag between $\delta^{18}O$ and density with $\delta^{18}O$ leading by 2 cm (T1) and 3 cm (T2). Such a difference would correspond to 1-2 months in time assuming equal accumulation over the year, but the shortness of the time series does not allow reliable estimate of the potential time lag.

In trench T2, we additionally show the mean ion-concentration profiles of MSA and Na^+, obtained from averaging over the four available profiles (Fig. 6c). Both ion profiles show a pronounced cyclicity and are anti-correlated to each other with peaks in MSA concentration corresponding to troughs in Na^+ concentration and vice versa (Table 2). The peaks in $\delta^{18}O$ are in phase with the ascending flanks in the MSA profile, and with the descending flanks of Na^+ concentration or almost within the trough. The peaks in the density profile are in phase with the peaks in MSA and the troughs in Na^+.

3.4 Spectral analysis of the vertical firn core density evolution

The four layers in the trench density dataset (Fig. 3), the reproducible density variations in the mean profiles, as well as the correlation with the $\delta^{18}O$ profile (Fig. 6) that is usually interpreted as a temperature signal, suggests that the density variations contain a seasonal signal. This is further supported by the observation that the layer thickness of around 20cm (Fig. 3) agrees with the annual accumulation rate at the site.

In a first view, this seems to contradict earlier findings [*Hörhold et al.*, 2012; *Freitag et al.*, 2013a] where it was shown that high-resolution density data in the top meters of the firn do not show any clear seasonality as diagnosed by analyzing the depth variability in the spectral domain. As these previous studies have been obtained at different sites and with different datasets, we repeat the wavelet analysis using the same methods as described in Hörhold et al., (2012) for the CT density data of all three firn cores. To be able to investigate variations in respect to time as the seasonal cycle, the depth scale is converted into water equivalent depth (w.eq.) and averaged to 5 mm w.eq. resolution. Low-frequency variations in the density records were removed using a finite impulse response high-pass filter [*Bloomfield*, 1976] (cut-off frequency 0.5 $(\text{m w.eq.})^{-1}$). The wavelet sample spectrum was estimated using the Morley wavelet (sowas package) [*Maraun and Kurths*, 2004] to analyze the depth dependent

behavior of the density in the frequency domain. Local significance was again tested against a red noise null hypothesis. The mean wavelet for all three cores is shown (Fig. 7) but similar results are obtained with any of the three cores. We note that this mean wavelet spectrum is a different quantity to that obtained by stacking the three cores first and than calculating the wavelet.

The result of the wavelet analysis (Fig. 7a) is very similar to the ones previously obtained from other Antarctic and Greenlandic cores [*Hörhold et al.*, 2012], showing a broad continuum of variability at the surface, a decrease in variability with a minimum around 10-20 m w.eq. and statistically significant patches of energy (black contours in Fig. 7a) appearing at depth close to the frequency of the modern accumulation rate range.

To complement the results of the wavelet analysis, we estimate the power spectra of the density variability of the firn cores at different depths (Fig. 7b) using the multitaper technique. Local significance was tested against a red-noise null hypothesis. The spectrum of the upper 10 m w.eq. of the core shows a variability continuum from the mm scale up to 0.3 m w.eq. length scale with increasing energy towards longer variations and no clear, statistically significant signal at the indicated present day accumulation rate. In contrast, the two other depth intervals show a distinct signal at the frequency of the accumulation rate. This in good agreement with former findings, where wavelet analysis revealed no distinct frequencies at the surface but a development of a significant peak at the frequency of accumulation rate with depth. We note that the statistically non-significant local maximum at the low frequency end of the spectrum (2-3 m w.eq.$^{-1}$) might be an artifact of the core processing as 1m pieces correspond to ~0.34 m w.eq. at the surface and more deeper in the core. Therefore, we can summarize that using spectral analysis no clear seasonal cycle can be detected in the near surface firn (upper 10m w.eq.) when analyzing single cores.

4 Discussion

We present an extensive high-resolution density dataset characterizing the near-surface density variability in an Antarctic low-accumulation region. In the following, we will discuss potential mechanisms for the build-up of the layered snow column, its link to the layered structure of compacted firn and the representativeness of single firn-core measurements.

4.1. Spatial variability of density in the upper snow column

The re-deposition due to interaction with wind is one of the reasons for the high lateral density-variability of surface snow [*Fisher et al.*, 1985; *Birnbaum et al.*, 2010; *Libois et al.*, 2015]. Our site is located within a region of light catabatic winds leading to a moderate mean snow density of 340 kg/m^3 [*Ligtenberg et al.*, 2011]. Here, snow is deposited in snowfields of several meter length with sporadic formations of barchan-type dunes of high density during strong wind events [*Birnbaum et al.*, 2010]. Below the surface, patches of high snow density in the trench (Fig. 3) suggest that these dunes have been buried and are a main cause for the lateral density variability. This confirms recent findings of a nearby 2D density profile [*Proksch et al.*, 2015].

While an earlier study investigating five shallow firn cores from the same region found that the dune horizons were randomly located within the cores [*Birnbaum et al.*, 2010], our data shows that the high-density regions are parts of continuous layers and thus cause at least part of the stratification. Both results are consistent given that the firn cores presented in Birnbaum et al., (2010) were spaced more than 50 m from each other and thus continuous layers would not have been detectable.

Wind-scoring can create a pronounced surface roughness on a daily time scale with an amplitude sometimes exceeding the annual accumulation rate [*Gow*, 1965; *Libois et al.*, 2015]. In our case, the surface undulations have peak-to-trough variations of 12 cm for trench T1 and 13 cm for T2 (Fig. 3). This represents a snapshot during the time of sampling and is less than the annual accumulation of about 20 cm of snow.

These undulation do not grow larger with time as evidenced by the fact that the surface looks similar from year to year. Earlier studies described dunes and sastrugi to be worn down by sublimation-deflation over the summer [*Gow*, 1965; *Benson*, 1971; *Palais*, 1984; *Mosley-Thompson et al.*, 1985]. Alternatively, a negative relationship between the actual height anomaly and the accumulation must exist: troughs get more accumulation than peaks. Both mechanisms could explain our finding that the layering at depth is on average horizontal and does not follow the modern snow-surface (Fig.3). Thus the meter to deca-meter surface undulations seem to be a seasonal phenomena, which get "reset" every year.

4.2. Representativeness of single vertical density profiles

The large lateral variability of density at our study site (Fig. 3) is also reflected in the poor correlation between different vertical density profiles and different firn cores. This is a typical finding for low-accumulation sites [*Palais*, 1984; *Jones et al.*, 2014] and also applies to other parameters such as oxygen isotopes [*Karlöf et al.*, 2006; *Muench et al.*, 2016]. The results are in strong contrast to Antarctic high accumulation sites e.g. at Law Dome in which single profiles seem to be representative over a an area of multiple kilometers [*McMorrow et al.*, 2002].

Going beyond showing the limitations of single profiles and firn cores, we could demonstrate the existence of a common signal across horizontal scales of at least 500 m as reflected in the strong correlation of the mean profiles from each trench. The strong increase in correlation, when analyzing averages across multiple profiles, shows that the horizontal scale of the depositional noise is considerably smaller than the length of the trenches yet larger than our lateral sample spacing. This is reflected in a lateral decorrelation length (Fig. 5) of less than 5 m. For future studies, this result suggests that in this region point measurements such as snow-stakes or firn cores should be placed at least 5 m from each other in order to avoid recording the same local depositional noise. It is important to note that our analysis was performed perpendicularly to the dune direction. Since the dunes are likely to determine the lateral scale of the local signal / depositional noise, the decorrelation length, and thus the optimal spacing to determine a representative signal, has to be larger in the dune direction because of the larger dimensions of dunes in wind direction.

The other approach to increase the representativeness of the signal is to vertically average the data. The effectiveness of this approach depends on the vertical correlation of the noise. Our finding that the surface undulations seem to be lost further down in the firn column is promising, but a more detailed analysis of the vertical correlation structure of the signal and the noise is needed in order to quantify the effects of vertical smoothing on the representativeness of the signal.

4.3. Seasonal cycle in snow density

The most prominent feature in our dataset is the horizontal layering of the density variations. The spacing of the layers of 15-25 cm, in line with a typical annual layer thickness of 20 cm (62-73 kg/m^2 accumulation per year/mean density of 340 kg/m^3) suggests that these are seasonal phenomena. This is supported by the similarity to the signal in the water isotopes, which is usually interpreted as being driven by the seasonal cycle in temperature (Fig. 6).

The ion concentrations of MSA and Na^+ are known to exhibit a seasonal cycle in the atmosphere over Kohnen station [*Weller and Wagenbach*, 2007], as well as a pronounced seasonal cycle in surface snow pits, firn core measurements [*Goektas et al.*, 2002] and in the deeper firn [*Sommer et al.*, 2000]. The timing of MSA peaks is in late summer to fall, for Na^+ in winter to spring [*Goektas et al.*, 2002; *Weller and Wagenbach*, 2007]. This seasonality is consistent with the observed phase relationships between density, impurities and isotopes (Fig. 6, Table 2), and it thus strongly supports that the average density profile shows a seasonal signal with maximum density around summer and minimum density around winter. We note that from previous published data from Antarctic and Greenland sites [*Benson*, 1971; *Etheridge et al.*, 1992; *Gerland et al.*, 1999] no clear definition of a relationship between season and high or low density can be drawn. Therefore, the representativity of our finding for other Antarctic sites is unclear.

In contrast to the clear seasonality in the average density profile, the seasonal cycle of density in single cores is weak and often not detectable (Fig. 4, Fig. 7). This can be attributed to two reasons. Firstly, the signal (approximated by the mean profile) is small relative to the total variability. Estimating the signal to noise ratio (SNR) from the correlation across profiles as R/(1-R) [*Fisher et al.*, 1985], only considering profiles separated by more than the decorrelation length of the noise (>5 m), results in a SNR of 0.15 (Table 2). Secondly, the accumulation rate shows a considerable inter-annual [*Oerter et al.*, 2000] and inter-decadal [*Klein*, 2014] variability. This distributes the energy across frequencies and thus inhibits the detection of the seasonal cycle even when analyzing longer density profiles. In contrast, given that the average accumulation rate over a region is uniform, averaging over space overcomes this problem and explains why horizontally integrating sensing techniques such as radar (but also the eye visually tracking horizons in snow-pits) see annual horizons [*Winebrenner et al.*, 2001; *Anschütz et al.*, 2007; *Eisen et al.*, 2008; *Arthern et al.*, 2013].

The most obvious reasons for seasonality in the density signal are seasonal variations of temperature, wind and radiation. They can affect the precipitation/deposition on the one hand, and post-depositional effects like snow metamorphism caused by temperature gradients or other destructive processes induced by radiation or wind on the other hand [*Alley*, 1988; *Harper and Bradford*, 2003]. However, very different observations are published regarding the time and season of low- or high-density snow deposition/formation, delivering an overall heterogeneous picture of snow seasonality on top of the ice sheets [*Gow*, 1965; *Palais*, 1984; *Alley*, 1988; *Li and Zwally*, 2002; *Birnbaum et al.*, 2010; *Fujita et al.*, 2014]. Given the contradicting evidences from the literature and the limited number of years covered by our dataset, we refrain from proposing a mechanistic understanding of the seasonal variations in density in this study. Nevertheless, we hope that our empirical finding of summer related to high density will foster new investigations on the seasonality of surface firn.

4.4. Density layering in firn and impurities

The density layering in deep firn is the result of a densification process acting on the layered snow with an increase in mean density by almost a factor of three in the top 100 m [*Freitag et al.*, 2013b]. Our new dataset proposes the existence of an annual cycle in density already in the top meter. However, the relative contribution of the seasonality to the total variability is small (<20%) which therefore does not allow the detection of the seasonal cycle in single cores. In contrast, analyzing the firn deeper than 30 m below the surface shows a stronger seasonal signal (relative to the total variability) (Fig. 7), confirming earlier findings [*Hörhold et al.*, 2012; *Freitag et al.*, 2013a].

To explain the stronger seasonal cycle in the deeper firn, two scenarios seem possible. First, the deep seasonal cycle might be an amplified version of the surface seasonal cycle of an earlier time. Therefore a driver with the same seasonal phasing or a selective densification mechanism would need to be invoked, which damps all variability but the seasonal cycle. Physical or microstructural properties of layers can be thought to be generated directly at the surface during deposition and favoring high densification rates in low density layers and low densification rates in high density layers [*Hörhold et al.*, 2012; *Fujita et al.*, 2014].

Second, the deep seasonal cycle might originate from processes independent from the surface seasonal cycle in density. For this hypothesis, another driver with a seasonal cycle, potentially with a different phasing that the surface density seasonality would be needed. It was proposed earlier, that impurity concentrations, might be this driver [*Hörhold et al.*, 2012; *Freitag et al.*, 2013a]. In this case the original properties of layers deposited at the surface are overprinted by post-depositional metamorphism depending on their impurity loading. Such an impurity effect on density is highly debated and the chemical species responsible for such an effect is not clear. At the Kohnen site the Ca++ ion concentration develops a strong correlation with density with depth, which suggests impurities with a comparable seasonal cycle as the Ca^{2+}concentration to be involved [*Freitag et al.*, 2013a]. At other sites no correlation between $Ca^{2+}$and density was found [*Buizert et al.*, 2015] or other species are discussed with respect to processes actually transferring the impurity load into a densification rate [*Fujita et al.*, 2014].

While the trench data are too limited to reach a definite conclusion, the available evidence from the phasing of impurities (Fig. 6, Table 2) argues for the second hypothesis. Earlier studies showed an in-phase relationship of Na^{+} with Ca^{2+} [*Sommer et al.*, 2000] as well as strong correlation of Ca^{2+} with density at greater depths at the Kohnen site [*Freitag et al.*, 2013a]. In the trench mean density profile, Na+ is out of phase with the density signal (Table 2), thus in contrast to the in-phase relationship expected at greater depths, suggesting a depth-dependent change of the density layering. This hypothesis is also consistent with the finding that the impurities in our dataset show a stronger seasonality than the density at the surface (Table 2).

The observed seasonal cycles in isotopes, density and impurities indicate that depositional and post-depositional processes at the surface are not strong enough to destroy the sub-annual order of buried snow layers at Kohnen. This allows for the possibility that seasonal properties are preserved that later lead to a lateral homogenization of density. We speculate that such layering in the deep firn could efficiently prevent the diffusive exchange of trapped air between adjacent layers near the bubble close-off.

5 Conclusions

An extensive density dataset from two trenches and three firn cores near Kohnen station, Antartica, allowed a detailed investigation of the lateral and vertical density variability in a low accumulation region. We find that the density variations of single firn profiles are not representative on seasonal to interannual timescales. However, averaging across multiple density profiles reveals a signal, at least representative on a 500 m scale. The analysis of oxygen isotopes and impurities, as well as the spacing of density layering, suggests that the average density signal is dominated by a seasonal cycle with summer related to higher densities.

It follows that at least in our study region, the contribution of the seasonal cycle to the total variability is strongly depending on the analyzed horizontal scale. In single snow pits or firn cores, stratigraphic noise dominates the variability and the seasonal cycle only explains a small part of the total variability. This masks the seasonal cycle and explains why previous firn-core studies reported a lack of a seasonal signal in Antarctica surface snow. Averaging over a larger region, for example by averaging across many firn cores or using horizontally integrating techniques such as radar data damps the stratigraphic noise and thus reveals the seasonal cycle. Measurements sensitive to the layering of the top meters of firn such microwave remote sensing or high-resolution radar altimetry, the lateral variability has to be taken into account when comparing these spatially integrating observations to firn cores.

Our findings of a seasonal cycle with maximum density in summer raise new questions on the genesis of physical properties at the surface of polar ice sheets and their fate with depth. While our dataset is too limited to draw definitive conclusions, it suggests that the seasonal cycle in density at the surface and the seasonal cycle in density at depth might be decoupled. This emphasizes the need to detangle the interaction of isotopic composition, density and impurities from the very beginning of the depositional and post-depositional processes in order to understand their linkage with depth and its meaning for the pore close-off.

Acknowledgments and Data

This study was part of the CoFiAP campaign (Coldest Firn Associated Projects) lead by the Alfred-Wegener-Institute, Helmholtz Center for Polar and Marine Research, which aims at a better understanding of the formation of the density and the isotopic signal in firn and ice cores. We thank all the scientists, technicians and the logistic support who worked at Kohnen station in the 2012/13 austral summer; especially Melanie Behrens, Tobias Binder, Andreas Frenzel, Katja Instenberg, Katharina Klein, Martin Schneebeli, Jan Tell and Stefanie Weissbach, for assistance in creating the trench dataset. We thank Katharina Klein for supplying the firn-core density dataset and Yuri Dvornikov for the GIS map. All numerical calculations were carried out using the software R: A Language and Environment for Statistical Computing. The data used are listed in the references and the PANGAEA repository at URL/DOI (link will follow). M.Hörhold was funded by the German Science Foundation Grant HO-5036/1-1. This work was supported by the Initiative and Networking Fund of the Helmholtz Association Grant VG-NH900.

References

Alley, R. B. (1988), Concerning the deposition and diagenesis of strata in polar firn, *J. Glaciol.*, *34*(118), 283–290.

Anschütz, H., O. Eisen, H. Oerter, D. Steinhage, and M. Scheinert (2007), Investigating small-scale variations of the recent accumulation rate in coastal Dronning Maud Land, East Antarctica, *Ann. Glaciol.*, *46*(1), 14–21, doi:10.3189/172756407782871756.

Arcone, S. A., V. B. Spikes, and G. S. Hamilton (2005), Phase structure of radar stratigraphic horizons within Antarctic firn, *Ann. Glaciol.*, *41*(1), 10–16, doi:10.3189/172756405781813267.

Arthern, R. J., J. Corr, H. F, F. Gillet‐Chaulet, R. L. Hawley, and E. M. Morris (2013), Inversion for the density‐depth profile of polar firn using a stepped‐frequency radar, *J. Geophys. Res. Earth Surf.*, *118*(3), 1257–1263, doi:10.1002/jgrf.20089.

Benson, C. S. (1971), Stratigraphic Studies in the Snow at Byrd Station, Antarctica, Compared with Similar Studies in Greenland, in *Antarctic Research Series*, edited by A. P. Crary, pp. 333–353, American Geophysical Union, Washington, D. C.

Bigler, M., A. Svensson, E. Kettner, P. Vallelonga, M. E. Nielsen, and J. P. Steffensen (2011), Optimization of high-resolution continuous flow analysis for transient climate signals in ice cores, *Environ. Sci. Technol.*, *45*(10), 4483–4489.

Birnbaum, G. et al. (2010), Strong-wind events and their influence on the formation of snow dunes: observations from Kohnen station, Dronning Maud Land, Antarctica, *J. Glaciol.*, *56*(199), 891–902.

Bloomfield, P. (1976), *Fourier Decomposition of Time Series: An Introduction*, John Wiley, New York.

Buizert, C. et al. (2015), The WAIS Divide deep ice core WD2014 chronology – Part 1: Methane synchronization (68–31 ka BP) and the gas age–ice age difference, *Clim. Past*, *11*(2), 153–173, doi:10.5194/cp-11-153-2015.

Denoth, A. (1989), Snow dielectric measurements, *Adv. Space Res.*, *9*(1), 233–243.

Eisen, O. et al. (2008), Ground-based measurements of spatial and temporal variability of snow accumulation in East Antarctica, *Rev. Geophys.*, *46*(2), RG2001, doi:10.1029/2006RG000218.

Etheridge, D. M., G. I. Pearman, and P. J. Fraser (1992), Changes in tropospheric methane between 1841 and 1978 from a high accumulation-rate Antarctic ice core, *Tellus B*, *44*(4), 282–294.

Fisher, D. A., N. Reeh, and H. B. Clausen (1985), Stratigraphic noise in time series derived from ice cores, *Ann. Glaciol.*, *7*, 76–83.

Freitag, J., S. Kipfstuhl, and T. Laepple (2013a), Core-scale radioscopic imaging: a new method reveals density-calcium link in Antarctic firn, *J. Glaciol.*, *59*(218), 1009–1014, doi:10.3189/2013JoG13J028.

Freitag, J., S. Kipfstuhl, T. Laepple, and F. Wilhelms (2013b), Impuritiy-controlled densification: a new model for stratified polar firn, *J. Glaciol.*, *59*(218), 1163–1169, doi:10.3189/2013JoG13J042.

Fujita, S., M. Hirabayashi, K. Goto-Azuma, R. Dallmayr, K. Satow, J. Zheng, and D. Dahl-Jensen (2014), Densification of layered firn of the ice sheet at NEEM, Greenland, *J. Glaciol.*, *60*(223), 905–921, doi:10.3189/2014JoG14J006.

Gerland, S., H. Oerter, J. Kipfstuhl, F. Wilhelms, H. Miller, and W. D. Miners (1999), Density log of a 181 m long ice core from Berkner Island, Antarctica, *Ann. Glaciol.*, *29*(1), 215–219, doi:10.3189/172756499781821427.

Glen, J. W., and J. G. Paren (1975), The electrical properties of snow and ice, *J. Glaciol.*, *15*, 15–38.

Goektas, F., H. Fischer, H. Oerter, R. Weller, S. Sommer, and H. Miller (2002), A glacio-chemical characterization of the new EPICA deep-drilling site on Amundsenisen, Dronning Maud Land, Antarctica, *Ann. Glaciol.*, *35*(1), 347–354.

Gow, A. J. (1965), On the accumulation and seasonal stratification of snow at the South Pole, *J. Glaciol.*, *5*, 467–477.

Gregory, S. A., M. A. Albert, and I. Baker (2014), Impact of physical properties and accumulation rate on pore close-off in layered firn, *The Cryosphere*, *8*, 91–105, doi:10.5194/tc-8-91-2014.

Harper, J. T., and J. H. Bradford (2003), Snow stratigraphy over a uniform depositional surface: spatial variability and measurement tools, *Cold Reg. Sci. Technol.*, *37*(3), 289–298, doi:10.1016/S0165-232X(03)00071-5.

Hörhold, M. W., T. Laepple, J. Freitag, M. Bigler, H. Fischer, and S. Kipfstuhl (2012), On the impact of impurities on the densification of polar firn, *Earth Planet. Sci. Lett.*, *325–326*, 93–99, doi:10.1016/j.epsl.2011.12.022.

Jones, T. R., J. W. C. White, and T. Popp (2014), Siple Dome shallow ice cores: a study in coastal dome microclimatology, *Clim Past*, *10*(3), 1253–1267, doi:10.5194/cp-10-1253-2014.

Karlöf, L., D. P. Winebrenner, and D. B. Percival (2006), How Representative Is a Time Series Derived from a Firn Core? A Study at a Low-accumulation Site on the Antarctic Plateau, *J. Geophys. Res.*, *111*(F4), doi:10.1029/2006JF000552.

Klein, K. (2014), Variability in dry Antarctic firn—Investigations on spatially distributed snow and firn samples from Dronning Maud Land, Antarctica, Staats-und Universitaetsbibliothek Bremen.

Kreutz, K. J., P. A. Mayewski, M. S. Twickler, S. I. Whitlow, J. W. C. White, C. A. Shuman, C. F. Raymond, H. Conway, and J. R. McConnell (1999), Seasonal variations of glaciochemical, isotopic and stratigraphic properties in Siple Dome (Antarctica) surface snow, *Ann. Glaciol.*, *29*(1), 38–44.

Landais, A. et al. (2006), Firn-air delta15N in modern polar sites and glacial-interglacial ice: a model-data mismatch during glacial periods in Antarctica?, *Quat. Sci. Rev.*, *25*, 49–62, doi:10.1016/j.quascirev.2005.06.007.

Li, J., and J. Zwally (2002), Modeled seasonal variations of firn density induced by steady-state surface air-temperature cycle, *Ann. Glaciol.*, *34*, 299–302.

Libois, Q., G. Picard, L. Arnaud, S. Morin, and E. Brun (2015), Modeling the impact of snow drift on the decameter-scale variability of snow properties on the Antarctic Plateau, *J. Geophys. Res. Atmospheres*, *119*, 11,662-11,681, doi:10.1002/2014JD022361.

Ligtenberg, S. R. M., M. M. Helsen, and M. R. van den Broeke (2011), An improved semi-empirical model for the densification of Antarctic firn, *The Cryosphere*, *5*(4), 809–819, doi:10.5194/tc-5-809-2011.

Looyenga, H. (1965), Dielectric constants of heterogeneous mixtures, *Physica*, *31*(3), 401–406, doi:10.1016/0031-8914(65)90045-5.

Maraun, D., and J. Kurths (2004), Cross wavelet analysis: significance testing and pitfalls, *Nonlinear Process. Geophys.*, *11*(4), 505–514.

Martinerie, P., D. Raynaud, D. M. Etheridge, J.-M. Barnola, and D. Mazaudier (1992), Physical and climatic parameters which influence the air content in polar ice, *Earth Planet. Sci. Lett.*, *112*(1–4), 1–13, doi:10.1016/0012-821X(92)90002-D.

McMorrow, A. J., M. A. J. Curran, T. D. Van Ommen, V. I. Morgan, and I. Allison (2002), Features of meteorological events preserved in a high-resolution Law Dome (East Antarctica) snow pit, *Ann. Glaciol.*, *35*(1), 463–470, doi:10.3189/172756402781816780.

Mitchell, L. E. et al. (2015), Observing and modeling the influence of layering on bubble trapping in polar firn, *J. Geophys. Res. Atmospheres*, *120*(6), 2014JD022766, doi:10.1002/2014JD022766.

Mosley-Thompson, E., P. D. Kruss, L. G. Thompson, M. Pourchet, and P. Grootes (1985), Snow stratigraphic record at South Pole: potential for paleoclimatic reconstruction, *Ann Glaciol*, *7*, 26–33.

Muench, T., S. Kipfstuhl, J. Freitag, H. Meyer, and T. Laepple (2016), Regional climate signal vs. local noise: a two-dimensional view of water isotopes in Antarctic firn at Kohnen Station, Dronning Maud Land, *Clim Past*, *12*(7), 1565–1581, doi:10.5194/cp-12-1565-2016.

Oerter, H., F. Wilhelms, F. Jung-Rothenhäusler, F. Göktas, H. Miller, W. Graf, and S. Sommer (2000), Accumulation rates in Dronning Maud Land, Antarctica, as revealed by dielectric-profiling measurements of shallow firn cores, *Ann. Glaciol.*, *30*(1), 27–34, doi:10.3189/172756400781820705.

Oerter, H., W. Graf, H. Meyer, and F. Wilhelms (2004), The EPICA ice core from Dronning Maud Land: first results from stable-isotope measurements, *Ann. Glaciol.*, *39*(1), 307–312.

Palais, J. M. (1984), *Snow Stratigraphic Investigations at Dome C, East Antarctica*, Institute of Polar Studies Report No. 78.

Proksch, M., H. Löwe, and M. Schneebeli (2015), Density, specific surface area, and correlation length of snow measured by high-resolution penetrometry, *J. Geophys. Res. Earth Surf.*, *120*(2), 2014JF003266, doi:10.1002/2014JF003266.

Rotschky, G., W. Rack, W. Dierking, and H. Oerter (2006), Retreiving Snowpack Properties and Accumulation Estimates From a Combination of SAR and Scatterometer Measurements, *IEEE Transcactions Geosci. Remote Sens.*, *44*(4), 943–956, doi:10.1109/TGRS.2005.862524.

Rott, H., K. Sturm, and H. Miller (1993), Active and passive microwave signatures of Antarctic firn by means of field measurements and satellite data, *Ann. Glaciol.*, *17*, 337–343.

Schwander, J., T. Sowers, J.-M. Barnola, T. Blunier, A. Fuchs, and B. Malaize (1997), Age scale of the air in the summit ice: Implications for glacial-interglacial temperature change, *J. Geophys. Res.*, *102*(D16), 19,483-19,493.

Sommer, S., D. Wagenbach, R. Mulvaney, and H. Fischer (2000), Glacio-chemical study spanning the past 2 kyr on three ice cores from Dronning Maud Land, Antarctica: 2. Seasonally resolved chemical records, *J. Geophys. Res. Atmospheres*, *105*(D24), 29423–29433, doi:10.1029/2000JD900450.

Svensson, A. et al. (2015), On the occurrence of annual layers in Dome Fuji ice core early Holocene ice, *Clim Past*, *11*(9), 1127–1137, doi:10.5194/cp-11-1127-2015.

Weller, R., and D. Wagenbach (2007), Year-round chemical aerosol records in continental Antarctica obtained by automatic samplings, *Tellus B*, *59*(4), doi:10.3402/tellusb.v59i4.17054.

Wilhelms, F. (1996), Leitfähigkeits-und Dichtemessung an Eisbohrkernen= Measuring the conductivity and density of ice cores, *Berichte Zur Polarforsch. Rep. Polar Res.*, *191*.

Wilhelms, F., J. Kipfstuhl, H. Miller, K. Heinloth, and J. Firestone (1998), Precise dielectric profiling of ice cores: a new device with improved guarding and its theory, *J. Glaciol.*, *44*, 171–174.

Winebrenner, D. P., R. J. Arthern, and C. A. Shuman (2001), Mapping Greenland accumulation rates using observations of thermal emission at 4.5‐cm wavelength, *J. Geophys. Res. Atmospheres*, *106*(D24), 33919–33934, doi:10.1029/2001JD900235.

Table 1. *Summary of the snow trenches analyzed in this study.*

Trench name	Position (NW End)	Bearing	Length sampled	#profiles
T1	75.00641SS, 0.074978E	140°N	45.6m	77
T2	75.00849S, 00.08693E	130°N	49.1m	83

Table 2. *Correlation, signal to noise ratio and relative phasing of the different parameters. Correlations for density (this study) and* $\delta^{18}O$ [*Muench et al.*, 2016] *are the mean values of both trenches whereas MSA and* Na^+ *(this study) were only measured in Trench 2. Lags were determined by cross-correlation with negative values indicating a lead relative to density. For* Na^+*, the maximum cross correlation for negative and positive lags are the same inside uncertainty; therefore both values are given.*

	Mean correlation R (>=10m distance)	Signal to Noise Ratio R/(1-R)	Lag to density in cm (~months)
Density	0.13	0.15	
$\delta^{18}O$	0.53	1.1	-3 cm (-2 month)
MSA	0.30	0.43	-1 cm (-1 month)
Na^+	0.31	0.45	9 cm / -10 cm (+5 / -6 month)

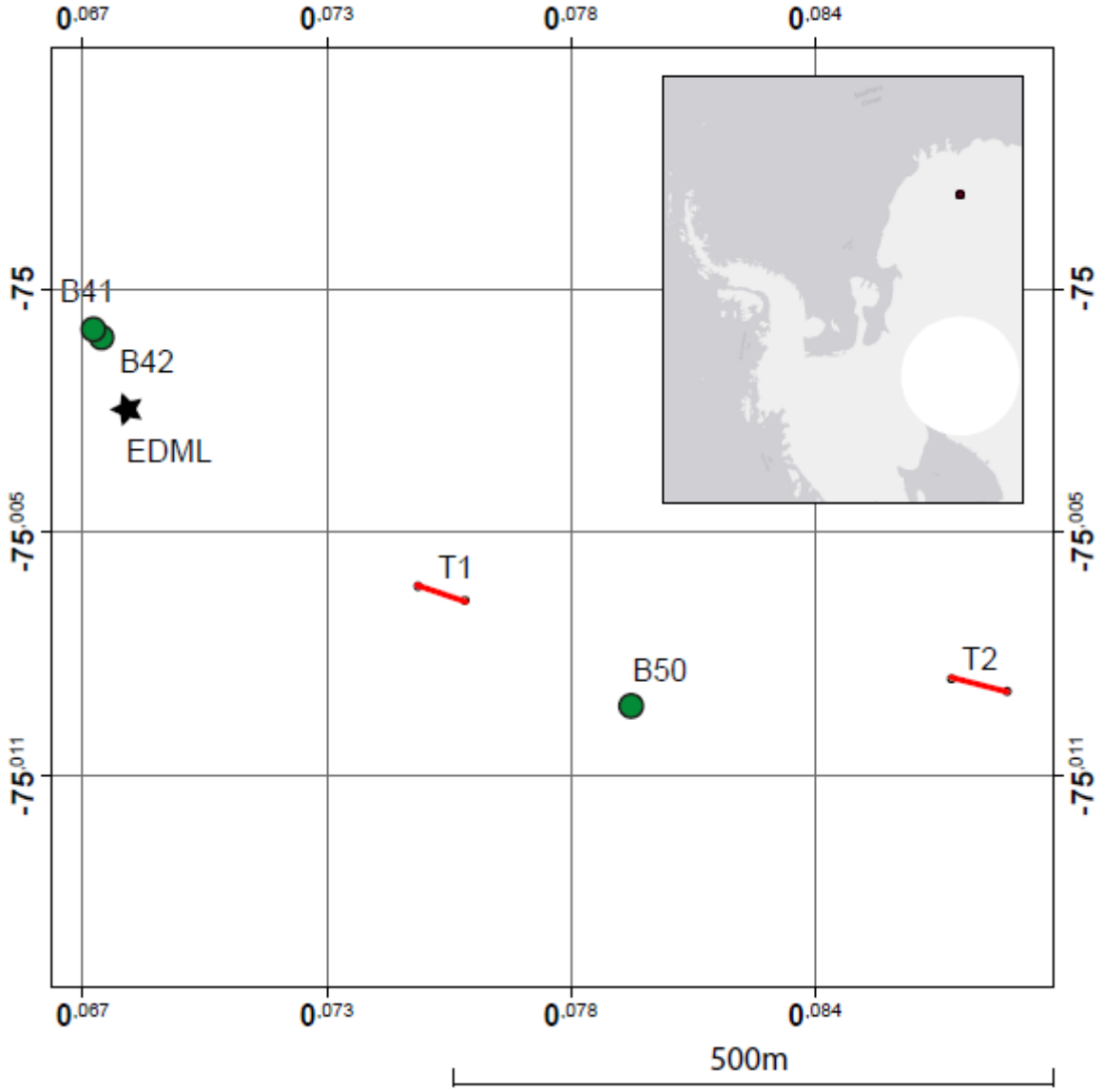

Figure 1. *Map of the firn core and snow trench positions. Firn core sites are shown as green filled circles, trenches as red lines. The drilling site of the EPICA Dronning Maud Land (EDML) ice-core is shown as black star.*

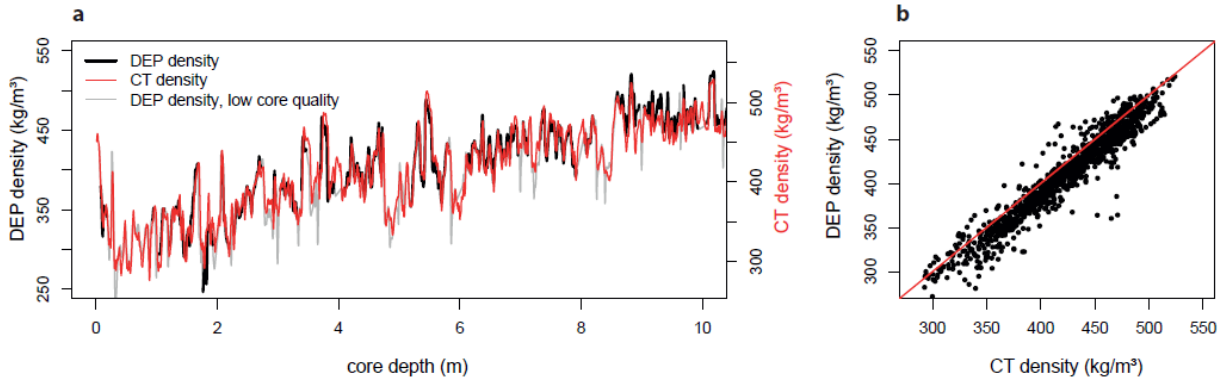

Figure 2. *Comparison of CT and DEP derived density of the top 10m of B41.* ***a*** *Comparison of the depth series. Grey shows the areas in which a low core quality was noted during the DEP measurements. Both axes have the same scaling.* ***b*** *Scatter plot of DEP vs. CT density. The 1:1 line is shown in red. Points with low core quality (= grey in left panel) are not included in the analysis.*

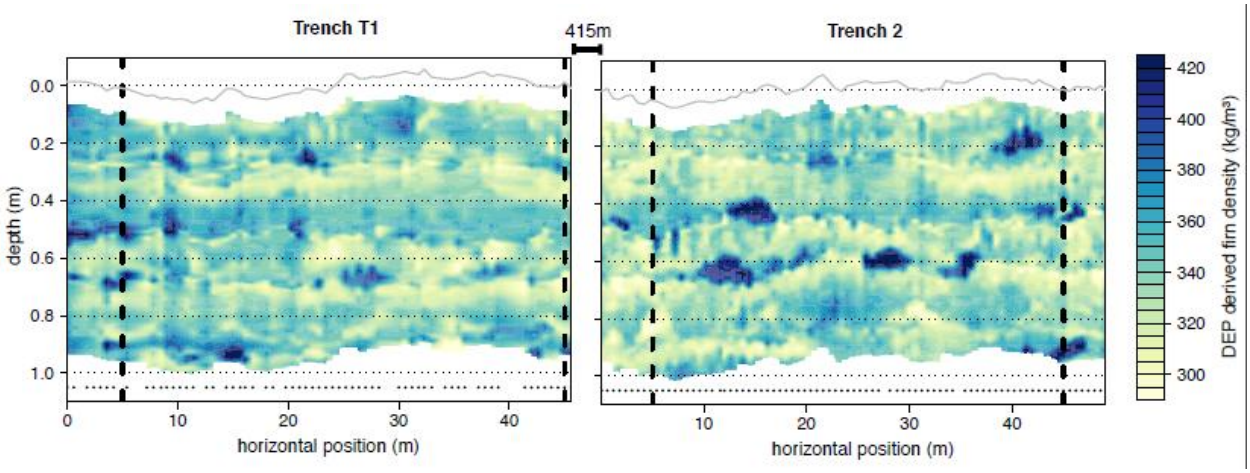

Figure 3. *2D (Vertical and horizontal) structure of the DEP derived density variations of both trenches. The depth is relative to an imaginary horizontal surface, which was arbitrarily set to 0 at the mean actual snow surface. The actual snow surface is shown as grey line. The removal of areas affected by edge effects in the DEP measurements lead to the missing area below the snow surface. Dots at the bottom of each panel depict where a profile was taken. Black lines indicate the positions of the profiles shown in Fig. 4. For displaying reasons, we limit the color scale to the 99% quantile range of the density variations.*

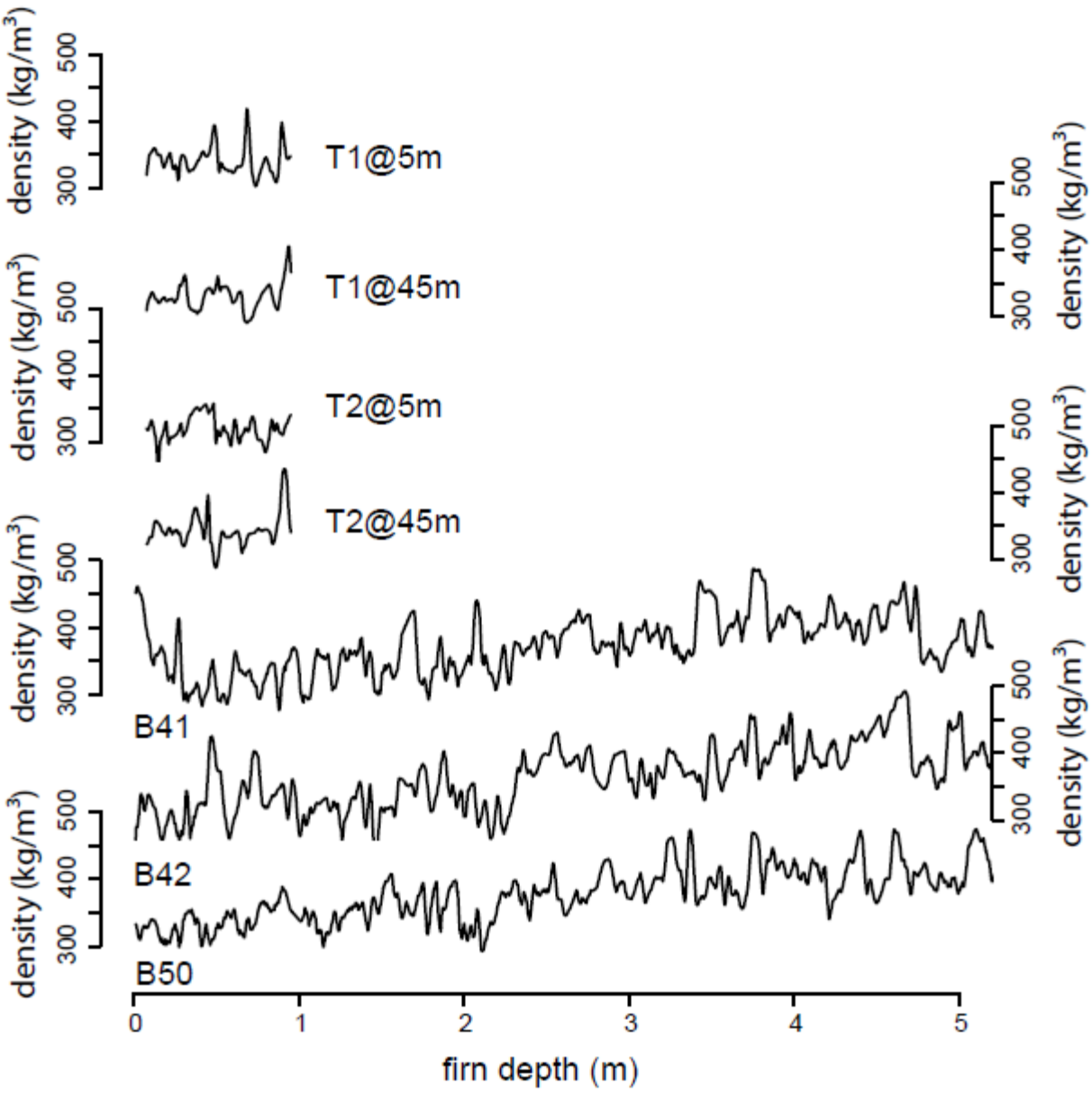

Figure 4. *Examples of vertical density profiles from the trench and firn core data. Shown are profiles from trench T1 at the horizontal position 5 and 45m, from T2 at 5 and 45 m and the top 5 m from firn cores B41, B42, B50. There is no significant correlation between any of the profiles (R<0.2 using detrended data).*

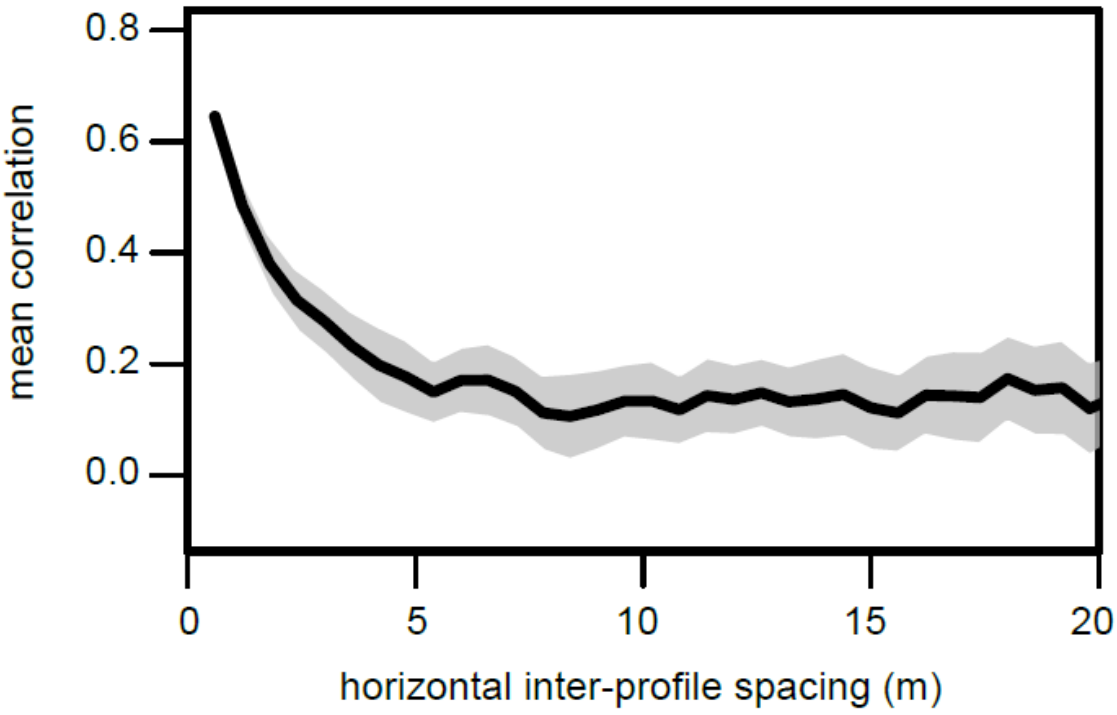

Figure 5. *Dependency of the density profile correlation on the horizontal separation distance between profiles. The mean correlation values of both trenches are shown. Nearby density profiles are highly correlated but this correlation decreases strongly in the first 5 m. Shading indicates the estimation uncertainty (2sd).*

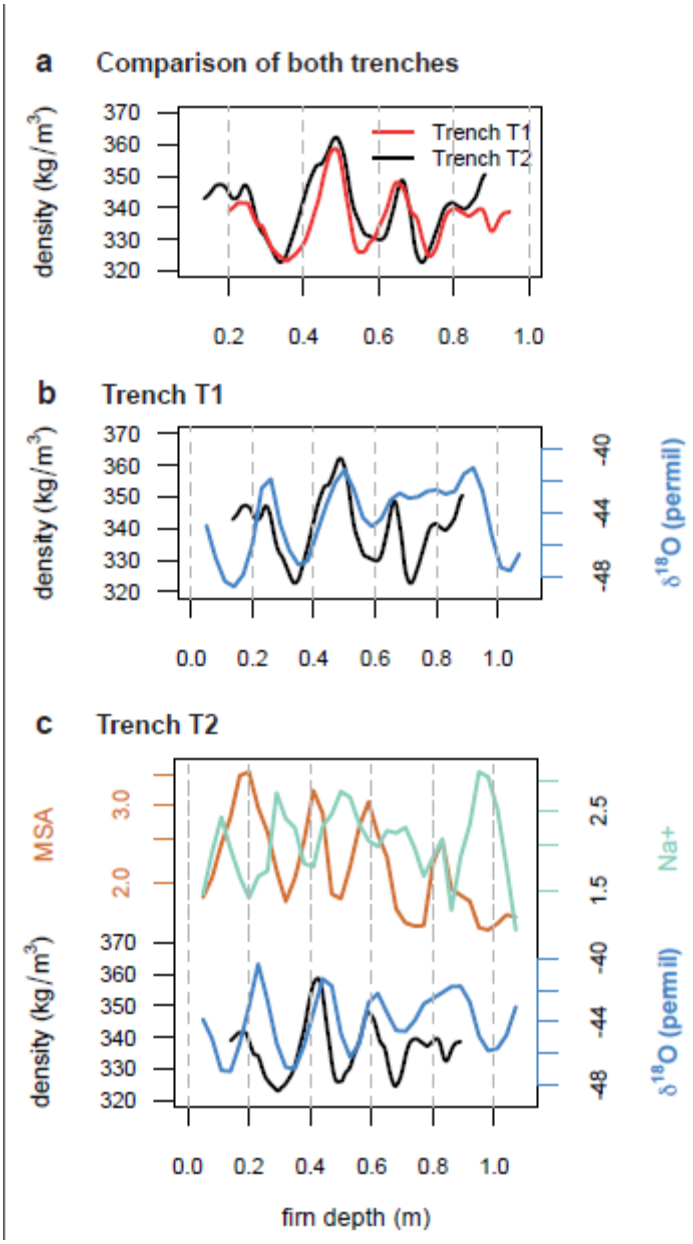

Figure 6. *Mean density profiles, mean isotope and mean impurity profiles.* ***a*** *Mean density profiles of Trench T1 and T2 (T2 shifted 6 cm) are highly correlated (R=0.84).* ***b-c****: Comparison of mean density and mean* $\delta^{18}O$ *profiles. In* ***c*** *in addition the mean impurity profiles are shown. The impurity concentration axes are on a logarithmic scale in ppb.*

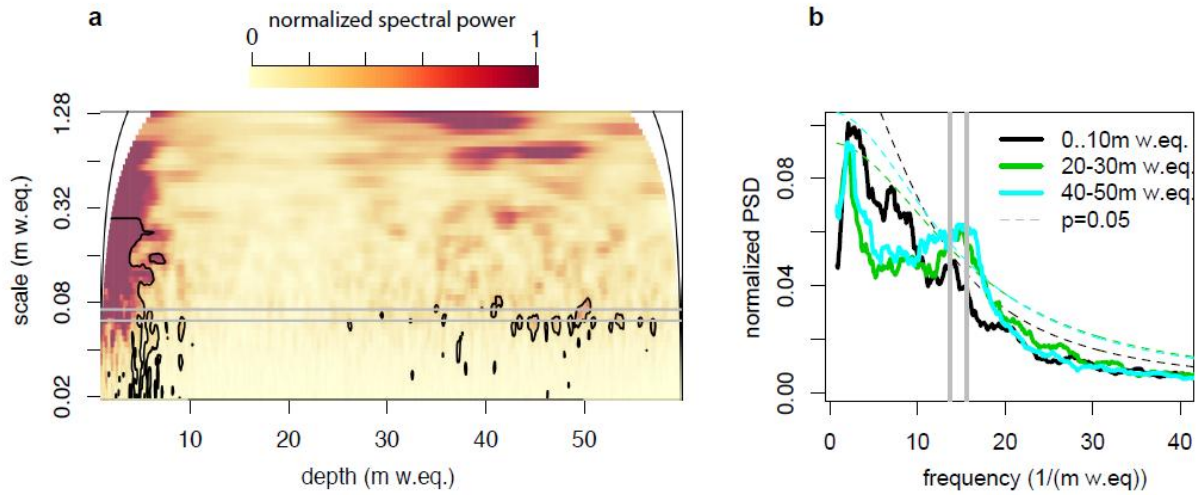

Figure 7. *Spectral analysis of the depth dependency of density variability.* **a** *Mean wavelet spectrum of the firn core density variations. Black contour lines enclose the regions with significant concentrations of spectral power.* **b** *Mean power spectra of density variations at three depth-intervals. Significance levels are shown as dashed lines. The approximate range of annual layer thickness is shown as horizontal grey lines in* ***a*** *and vertical grey lines in* ***b****. Significance (p=0.05) in* ***a*** *and* ***b*** *tested assuming a first-order autoregressive (AR(1)) model.*